CHALMERS
UNIVERSITY OF TECHNOLOGY

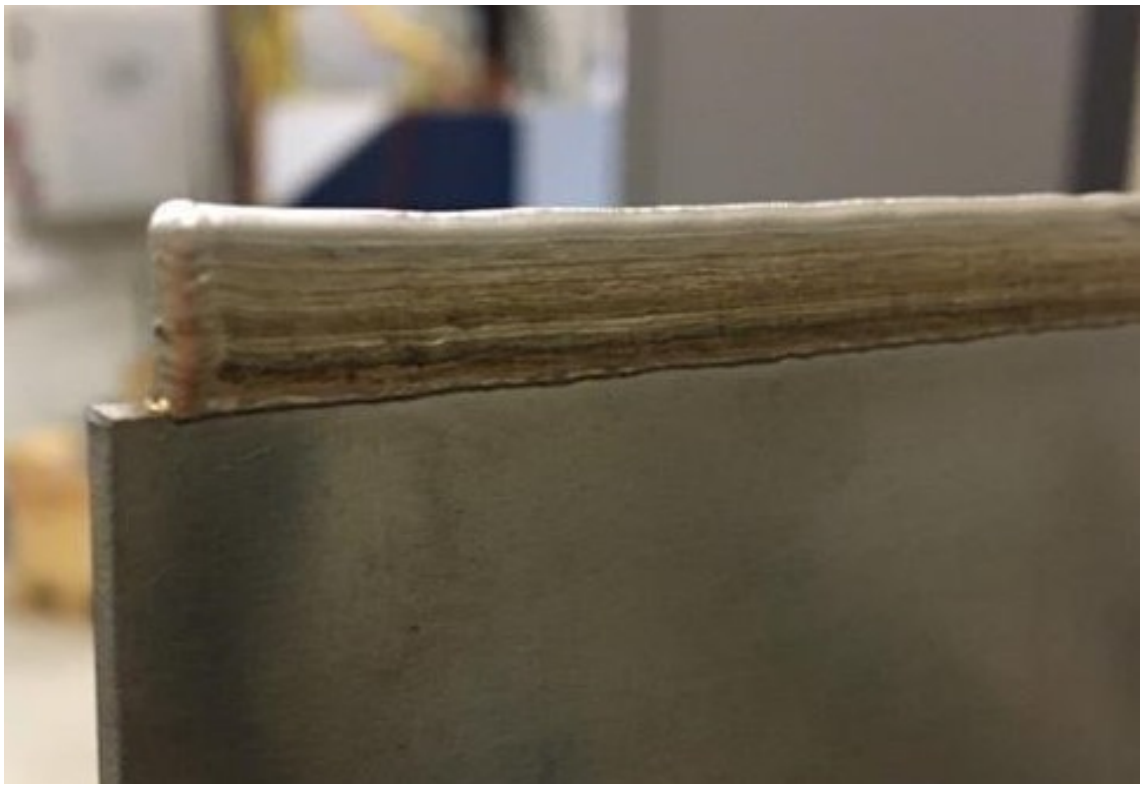

Development of high resolution Laser Wire Directed Energy Deposition

A novel approach to repair jet engine turbine blades

Master's thesis in Production Engineering

DAVID JOHANSSON
ERIK TJÄRDAHL

INDUSTRIAL AND MATERIALS SCIENCE

Production engineering
CHALMERS UNIVERSITY OF TECHNOLOGY
Gothenburg, Sweden 2022
www.chalmers.se

MASTER'S THESIS IMSX30

Development of high resolution Laser Wire Directed Energy Deposition

A novel approach to repair jet engine turbine blades

Master's thesis in Production Engineering

DAVID JOHANSSON
ERIK TJÄRDAHL

Industrial and Materials Science

Production engineering

CHALMERS UNIVERSITY OF TECHNOLOGY

Gothenburg, Sweden 2022

Development of high resolution Laser Wire Directed Energy Deposition
A novel approach to repair jet engine turbine blades
DAVID JOHANSSON
ERIK TJÄRDAHL

Supervisor: Almir Heralic

Examiner: Eduard Hryha

Master's thesis IMSX30
Industrial and Materials Science
Production engineering
Chalmers University of Technology
SE-412 96 Gothenburg
Sweden
Telephone: +46 (0)31-772 1000

Colophon:
The thesis was created using LaTeX

Cover:
Dual bead layers built on supported edge

Gothenburg, Sweden 2022

Development of high resolution Laser Wire Directed Energy Deposition
A novel approach to repair jet engine turbine blades
Master's thesis in Production Engineering
DAVID JOHANSSON
ERIK TJÄRDAHL
Industrial and Materials Science
Production engineering
Chalmers University of Technology

ABSTRACT

Among metal AM processes today, Laser Wire Directed Energy Deposition (Lw-DED) stands out as one promising technology for repair due to the high deposition rate, material efficiency, and good material properties, however, with relatively low resolution. Thus, there is a growing interest within industry to improve the resolution of the process in order to enable repair and manufacturing of smaller components without giving up the process advantages.

This report describes the considerations and steps taken to design, produce, and evaluate a fine resolution Lw-DED tool. The tool features a set of linear axis coupled to a robotic arm used for fine control of the melt. The tool also features a variety of sensors which combined allow for implementing automatic control loops to avoid process issues.

Tool evaluation was conducted by building thin walls on the edges of metal plates and bars on the face of plates. The built geometries were then inspected to compare to the net shape volume of the desired geometry and examined for lack of fusion defects. The test pieces produced with the tool were then compared against pieces produced with a more conventionally sized Lw-DED system.

The tool demonstrates the ability to produce fully dense parts with a wall thickness of 1.6 mm and a layer height of 0.2 mm in 308 stainless steel. Thus enabling repair of components such as jet turbine blades or creation of miniature cooling channels on heat exchangers.

Keywords: Lw-DED, AM, Additive Manufacturing, Fan blade repair, Aerospace, Cladding, High resolution

ACKNOWLEDGEMENTS

For their continuous help and expertise we want to thank our supervisors Almir Heralic and Petter Hagqvist. Their knowledge and insight has been a key part to enabling the thesis to reach completion. We also want to thank their company Procada for offering the thesis work.

For his advice and feedback during the thesis, but also for teaching the prerequisite knowledge from his course in additive manufacturing, we want to thank our examiner Eduard Hryha.

We want to thank CAM2 at Chalmers, and Högskolan Väst for their accommodations.

For helping out with some of our manufacturing as well as teaching us the machines in the workshop at the premises we want to thank Jonas Olsson.

TABLE OF CONTENTS

List of Figures

List of Tables

SPECIAL TERMS

Lack Of Fusion When depositing material on top of a substrate, the new material might not create a proper bond with the substrate. This can be due to the substrate being too cold, contamination on the surface, impurities or poor wetting. The result is a crack or gap between layers as they have not fused correctly.

Net shape The ideal geometry to be produced.

Stubbing The act of the wire penetrating the melt pool without melting, hitting the substrate below.

Tool Center Point A point defined in space on an industrial robot to be the center of motion, for example the laser focus point. All motion done by the robot will then be in relation to this point when positioning.

Undercut Depositing layers on top of each other causes a small portion of the layer below to remelt. This can cause the melt pool to create a recessed feature as the layer below adheres to the layer above creating a lack of material.

I. Introduction

In recent years the world of additive manufacturing (AM) has seen a boom in interest, investment, and developments, with new technologies and improvements constantly popping up. Industries in the forefront include medical, dental and aerospace [1].

The aerospace industry is very interested in the capabilities of additive manufacturing to reduce lead time, weight and cost of new parts. The industry also see a potential of AM in the repair of used parts like turbine blades [2], [1]. For reparation of blades, a promising AM technology is Laser-wire Directed Energy Deposition (Lw-DED) which is capable of depositing material directly onto existing parts. However, a current limitation of this technology is building on thin parts. These issues has its roots in difficulty in reducing layer thickness, fine motion control, and energy input. These challenges needs to be overcome before mainstream adoption in industry.

A. Background

Lw-DED is today present in production of structural parts for aircraft and rocket engine applications due to their rapid deposition rate and quality compared to competing technologies [1] [2]. Procada is a recently established company that has developed a novel way of controlling the Lw-DED process based on continuous process feedback through the wire filler material itself [3]. This permits full automation of the DED process such that material integrity can be guaranteed even for critical applications that were previously not feasible for the process. To this point, Procada has so far only implemented the laser-wire DED process for large scale features in the order of meters. Now Procada is looking to scale down this process to sub-millimeter applications such as repair of the leading edge of thin turbine blades used in jet engines.

B. Delimitations

- The thesis will not to much of an extent address the laser system nor the optics used, however they are a core element in the machine.
- The thesis will neither address programming and tool paths for the robots and control systems.
- The thesis will not feature an implementation of automatic control loops.
- Metallurgy is an important part of wire DED however material properties are beyond the scope of this report.

C. Process description

DED is an additive manufacturing technology were thermal energy is used to join material onto a substrate in order to build up a geometry. Key defining features of this technology is the high build rate compared to competing technologies, ability to deposit on existing parts, and large build volumes [4].

There exist multiple technologies in the DED family, the main difference between the existing technologies is what filler material and energy source they use. The most prevalent filler materials are powder and wire. Powder based DED use a fine powder that is blown onto the substrate and melt using, for example, a laser. Wire DED instead uses a wire as the filler material which is fed into a melt pool, similar to using a MIG welder. Wire DED is a process that is 100 % efficient in feed stock

usage as all fed material is used as opposed to powder DED which features less than 100 % feed stock efficiency [5].

When it comes to heat sources there are several to choose from. As long as energy can be directly transferred onto the surface to create a melt pool, a DED process can be performed. Examples of energy sources are, but not limited to, laser, electron beam, plasma arc, and metal arc. Combining these different types of filler materials and energy sources results in a few different available technologies such as Wire Arc Additive Manufacturing (WAAM), Electron Beam Additive Manufacturing (EBAM), Laser Metal Deposition (LMD), and Laser wire Directed Energy Deposition (Lw-DED). This report will focus on Lw-DED.

Lw-DED is used when you want a fast deposition rate, fully dense parts, and a high material utilization. The deposition rate of wire laser DED is typically in the range of kilograms/hour.

In Fig. 1, a schematic view of the Lw-DED process can be seen. The laser optics and wire feeder are moved together in order to create a solidified metal layer on top of the substrate, or the previous layer. The majority of the energy to join the layers together comes from the laser. In addition, the wire also has an electrical current running though it to soften the wire, a technique called hot-wire. By measuring the current, the conductance between the wire and substrate can be calculated[6]. This conductance value is then used in a regulator that adjusts the height of the wire in order to maintain process stability.

Key parameters to keep track of in Lw-DED is the laser power, surface speed, wire feed rate, hot-wire current and target conductance. These parameters become increasingly important when it comes to small, or thin, features as the smaller size decreases the size of the process window. Moving outside of the process window can cause the added feature to become deformed from interrupted mass flow in the form of droplet formation [7]. Alternatively, the added layer can experience lack of fusion due to too low heat input.

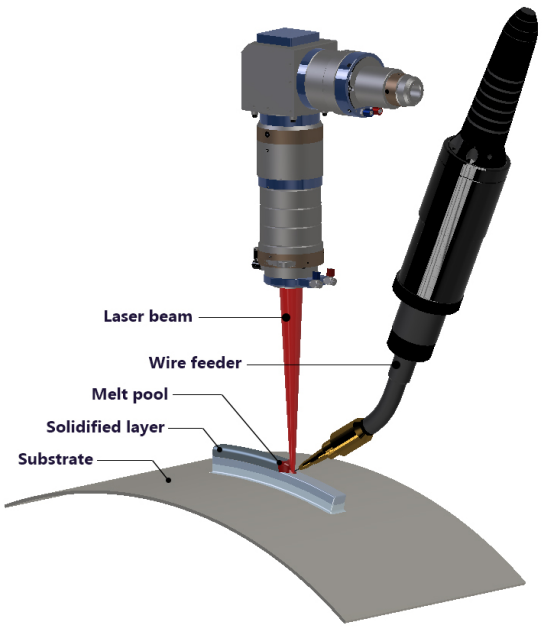

Fig. 1. A schematic image of the principle of wire laser DED. Image adapted from [3]

The wire should hit the melt pool close to the center of the laser spot to allow the laser to pre-heat the wire, allowing for a smooth and uninterrupted process. In Fig. 4, too much heat has been absorbed by the wire and the surface tension of the melted metal causes a droplet to form on the tip of the wire [7]. This droplet will continue to grow as it absorbs energy until gravity pulls it down, this droplet formation will cause an interrupted mass flow which can lead to defects. Having too little input energy in relation to mass flow will cause the wire to not properly melt and cause lack of fusion defects or lead to stubbing. The feed rate of the machine is also an important factor as moving too slow will cause heat to build up. This increases the possibility of the melt pool becoming unstable by boiling or melting multiple layers.

In Fig. 2, a snapshot of good process performance can be viewed. The wire forms a neck shape when it approaches the melt pool, which indicates that the wire melts as it enters the laser spot, while the surface tension pulls it into the melt. This behaviour indicates that the mass-flow and energy balance are correctly tuned. The laser also partially remelts the directly adjacent layers allowing for the beads to join correctly, generating a defect free product. If the distance between the laid beads were to increase, the beads will not properly join as the heat input from the laser into the adjacent beads is too low, resulting in lack of fusion. These defects that can occur can be seen in Fig. 3 and 14 where two beads have separated. This effect can be partially counteracted by angling the laser into the previous layer by a few degrees allowing the laser energy to better be absorbed into the directly adjacent layers as seen in Fig. 5.

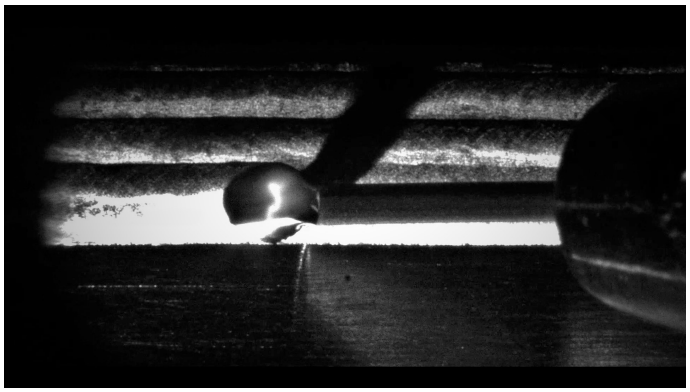

Fig. 2. Process image of desired process performance. The wire is fed from the right into the melt pool in the center. Wire diameter is 0.8 mm. Feed direction is from left to right.

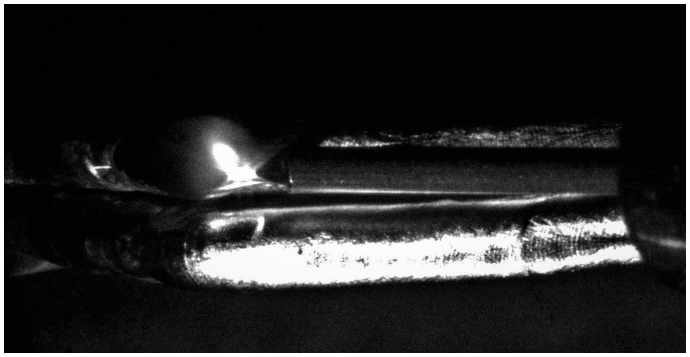

Fig. 3. Image of a dual bead process were the top and bottom layer experiences a lack of fusion. The melt does not extend between the beads thus leaving an air gap. Feed direction is from left to right.

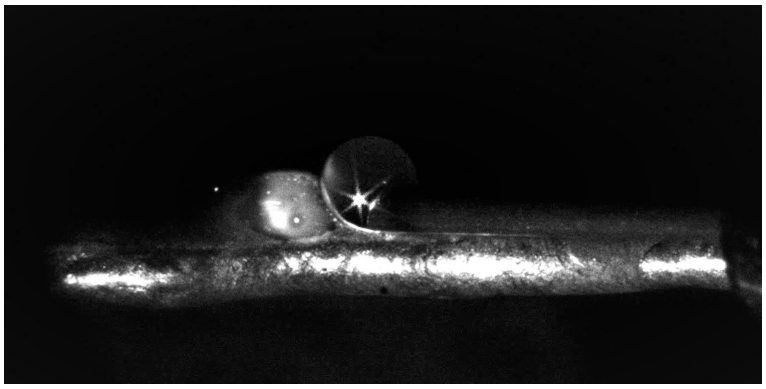

Fig. 4. Image of a droplet forming on the tip of the wire. The droplet holds itself to the wire by surface tension until gravity pulls it down. Feed direction is from left to right.

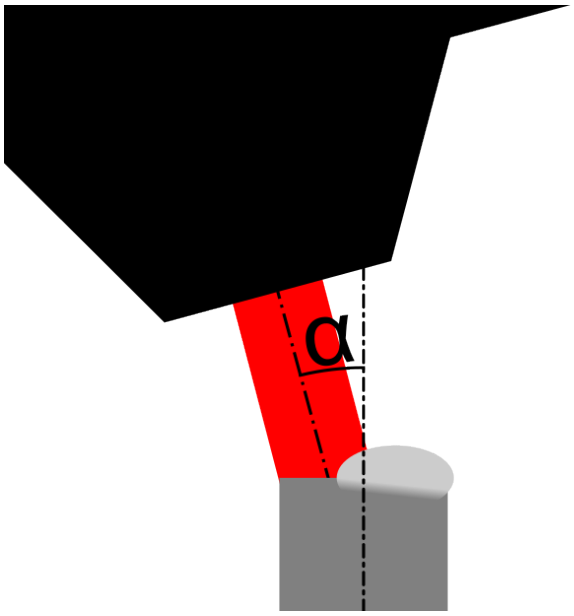

Fig. 5. Schematic image of angled laser optics to better focus the heat energy into the corner of the beads

In addition to the laser angle in relation to the substrate, there is also the consideration of the angle and positioning of the wire relative to the deposition direction as illustrated in Fig. 6 with three defined feeding types. Which of the feeding types is most suitable depends on the material and laser type. However, when melting Ti- or Ni-based alloys, a front or side feeding is seen to produce preferable results over back feeding [8].

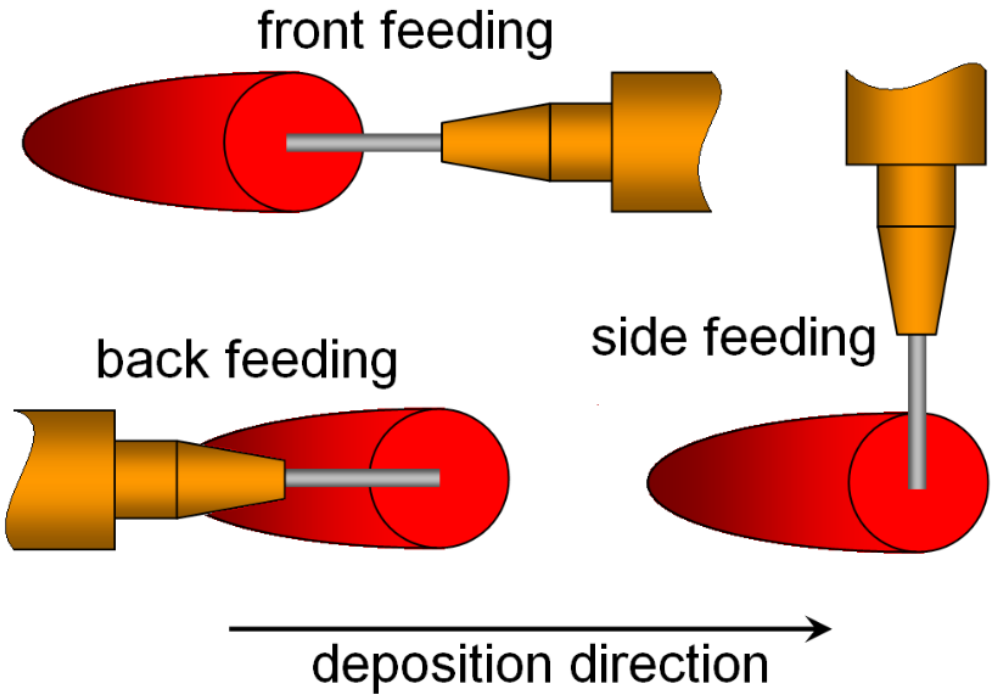

Fig. 6. Illustration showing the positioning of the wire in relation to the deposition direction. Image cortesy of Dr Almir Heralic, adapted from [7]

D. Problem description

In order to repair jet engine turbine blades there is a need to repair smaller features than is currently possible with Lw-DED. Blades of jet engine turbines have a small cross-section of ≈ 1.1 mm [2]. In order to build these smaller features, the laser spot size needs to get smaller to allow for thinner layer widths. In addition, the wire needs to get smaller in order to keep an advantageous size ratio with the spot size. As an effect, the scale of movements also decreases.

When building small features in the range of a few millimeters to sub millimeters, the allowed error for the position of the wire in relation to the spot is greatly reduced compared to larger scale processes. As the wire diameter is reduced, the compliance increases which can lead to excessive bending when stubbing. In addition, the wire has a certain curvature due to being stored in spools. This inherent curvature causes the wire to wander in relation to the melt as it gets fed. A little movement would be allowed, but allowing the wire to move outside of laser spot can cause the nozzle and wire to deflect away. This can cause an runaway reaction causing even more deflection until the wire in its entirety is outside of the laser spot as shown in Fig. 7. Allowing the wire to runaway will cause poor surface finish, as this is a disruption in the process it can also cause lack of fusion if not handled in next coming layers. Thus, the wire cannot simply be fixed in relation to the laser spot. By controlling the wire in the XY-plane this curvature and compliance can be compensated for in real time allowing for a consistent process.

Fig. 7. Process image of a runaway wire. The wire is fed from the right into the melt pool in the center of the image. The wire has deflected downwards in the image resulting in an interrupted process flow. Feed direction is from left to right.

When building thin walls with Lw-DED, an undercut between the deposited layer and the substrate might form, resulting in missing material relative to net shape. To compensate for this undercut, multiple beads can be deposited next to each other allowing for excess of material on the sides that can later be machined [2]. Having a low positional accuracy in this process can cause the laser spot to lie too much to one side leading to poor wetting between the beads and thus lack of fusion. This issue can be addressed by allowing for better positional accuracy.

These presented issues comes down to the desire for 100 % density parts with no defects. A single fusion defect or inclusion is unacceptable when performing turbine blade repair. These parts are subject to high cyclic stresses hence fatigue strength must be ensured [2]. Even though Lw-DED generates fully dense parts and is capable of depositing on existing parts, a process disturbance causing a lack of fusion could introduce voids, gaps, or other defects in the part.

II. METHOD

The method section of this report is divided into three subsections: design, manufacturing and testing. These sections describe how, and why, the different parts were developed.

A. Tool Design

The first step to evaluating a miniaturised wire DED system was done by creating a project specification and evaluating different solutions. The project specification contains the system requirements, and preferred system capabilities as seen in Table I. This way, a methodical selection was achieved. It is key that this selection is done early in the process since, during the time period of the thesis work, there are significant lead times on many industrial components internationally.

TABLE I
TABLE OF PROJECT REQUIREMENTS AND DESIRED PERFORMANCE.

	Minimum requirements	Preferred Performance	Comment
Wire-Z-envelope	6 mm	20 mm	Height adjustment for the wire
Laser-Y-envelope	5 mm	10 mm	Allowing the laser to better track the path
Wire-XY-envelope	5 mm	10 mm	Envelope as a diameter circle
Wire Acceleration in XY-plane	10 mm/s^2		Acceleration/retardation of the wireholder in the XY-plane
Wire Acceleration in Z-axis	5000 mm/s^2		Acceleration/retardation of the wireholder in the Z-plane
Payload	0.5 kg or weight of wire holder assembly		
Rotation around Z-axis	180°	270°	The rotation of the wireholder around Z (C-rotation)
Wire degrees of freedom	4 DOF (XYZ-C)	6 DOF (XYZ-ABC)	Total amount of DOF for the wireholder
Laser degrees of freedom	1 DOF (Y)		Total amount of DOF for the laser
Accessibility			The tool should be able to reach narrow areas

The evaluation step is conducted as follows: a concept is created from an idea and then a mock up is modeled and evaluated based on the different criteria defined in the specification. The criteria minimum requirements is something that must be achieved in order to have a functional system. As multiple solutions will be able to achieve the minimum requirements the preferred performance is set up to pick the best one of the evaluated systems.

The resulting solution is then refined until a producible prototype is achieved. The refinement contains not just representative CAD models of all parts but also mathematical models, and Bill of Materials (BoM). The system is then manufactured and evaluated in a robot laser welding cell.

1) Current implementation: In the current implementation of the wire DED system, the tool consisting of a laser source and wire feeder is mounted on an industrial robot arm. The robot arm handles the movements relative to the substrate allowing for easy programming of tool paths in the provided environment. Setting the robot's Tool Center Point (TCP) at the laser focus allows for millimeter precision positioning with little effort. The wire in this implementation has one degree of freedom (DOF), the height relative to the substrate.

As some materials are sensitive to oxides and other atmospheric contamination, an inert atmosphere was needed. This is provided by enclosing the process in a plastic 'tent' and filling it with argon. The tent is flexible to allow motion and attached to the build plate and tool so the argon won't escape.

2) Proposed solution: The proposed solution utilizes the fact that an industrial robot already is installed and integrated in the existing environment. The realised problem solution aims to provide a fine control system as the end-effector of a robot arm.

To address issues with the positional accuracy orthogonal to the seam (y-axis), an actuated axis was needed to ensure that the laser properly tracks the seam. In addition to this, a manipulator for controlling the wire relative to the laser was necessary. This was required to ensure the wire hit the melt pool in a preferential spot in order ensure surface quality [9]. Reachability was also a concern when creating the Lw-DED tool as the features to be repaired can be hard to reach. The designed tool must therefore allow the laser to hit the substrate at an advantageous angle all while minimising the influence of gravity in the melt pool.

Given the considerations above, and that side to side angle adjustment is more important than front to back angle adjustment, in the case of fans blade repair, the front feeding direction as shown in Fig. 6 was chosen. This gives us a wedge shape in the travel direction allowing for excellent reachability.

The laser spot was coupled to the wire by the seam following actuator as both need to track the seam at the same speed. To move the wire relative to the laser spot, a three axis Cartesian system was implemented. A camera providing a view of the melt pool in the XY-plane was mounted coaxial to the laser. This also supports future implementation of a Computer Vision control loop, allowing to autonomously correct the position in the XY-plane.

Another problem the kinematics needs to address is the wire sticking to the melt pool at the end of a seam as the melt pool solidifies. To achieve this, the wire needs to be capable of rapidly lifting up from the substrate. However, another issue that can arise from this maneuver is a molten bead stuck to the tip of the wire getting flung off and potentially damaging equipment. To avoid this, the x- and z-axis motors will work together to do a diagonal move instead of just one axis moving. This will give the maneuver a $\sqrt{2}$ times increase in speed coupled with a simultaneous retraction of the wire.

Positioning systems The fine motion control system is implemented as follows. A linear actuator controls the position of both the laser spot and the wire in relation to the robot's TCP. This will allow the laser spot to better follow a tool path in small dimensions, compensating for poor robot resolution. The wire is tethered to these adjustments as the wire should remain in the laser spot to ensure a proper process.

Sensors The tool makes use of sensor input in order to detect and compensate for variables that lead to issues such as undercutting, stubbing, and lack of fusion.

B. Manufacturing

During the design phase of parts, the main method of producing prototypes were done with polymer additive manufacturing using fused filament fabrication (FFF) to confirm that the parts would be possible to install, fit together, and allow access to downstream parts. When a design was considered done and tested it was mainly manufactured in aluminum and steel using an abrasive water jet. Most of the parts were also further refined with manual machining to compensate for the initial rough cutouts. The final assembly can be seen in Fig. 18 in the appendix.

Some parts that were not at high risk of excessive heat were kept as polymer parts printed in Acrylonitrile-styrene-acrylate (ASA). This material was chosen due to its heat deflection temperature of 92 °C and glass transition temperature of 112 °C.

There was also a need for a fine threaded M5 rod to refit the initially manual linear axis to belt drive with stepper motors. This rod has a pitch of 0.5 mm/rev resulting in a linear translation

resolution range from 0.01 μm to 2.5 μm at 256 microstepping to no microstepping, respectively, with the selected stepper motors. However, as the available torque decreases non-linearly with higher microstepping [10], and the steps get rougher at lower microstepping, a balance had to be found. For our use case 8 microsteps was found to give sufficient resolution with acceptable step roughness and torque. Due to drive backlash and control loop limitations the effective resolution of the axis were around 50 μm.

Base plate An aluminum plate together with some struts acts as the interface between the robot arm and the laser fixture. This plate acts as a mounting system for the wire feeder and houses some of the electronics in order to minimize wire routing outside the tool. This minimises the risk that wires can get tangled in the robot arm. This is achieved by having two struts connect in an L-shape and a third strut act as leverage support connected to the base-plate and robot arm as seen in Fig. 8.

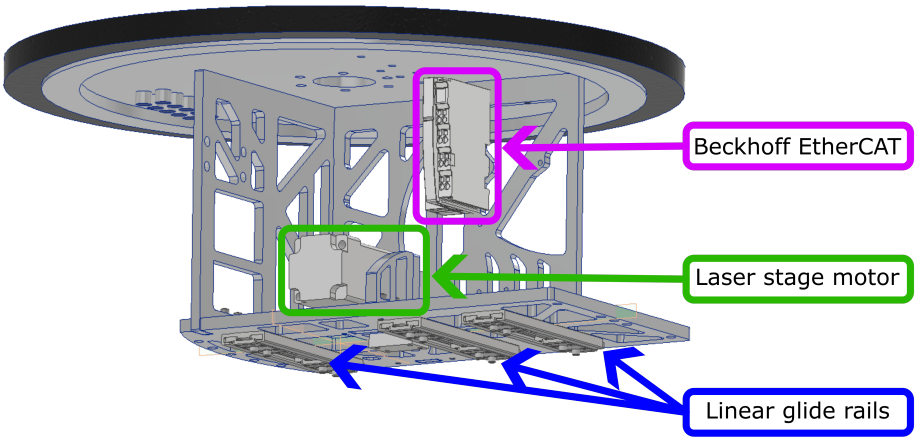

Fig. 8. A CAD image depicting the base plate and three struts. Also seen in the image is the laser stage motor, three linear glide rails, and a Beckhoff EtherCAT® module.

Laser fixture The base plate has linear guide rails and a linear motor mounted to the laser fixture. This axis is used to control both the laser spot and wire together, allowing for proper seam following. The laser fixture is designed to hold the laser optics, linear wire axis, and auxiliary components. This plate, seen in Fig. 9, was initially designed with consideration for a rotational axis for the wire control but was left out due to sourcing issues. Instead the holes were repurposed for mounting extra components. Both this plate and the base-plate has a cutout for a camera module attached to the laser giving a video feed coaxially with the laser beam.

For mounting the Laser to this fixture, a C-clamp was cut with water-jet and an adapter-plate CNC-milled. This gives fixture connections close to the output as well as the input without much interference with the rest of the system. These two fixtures can be seen with the laser optics in Fig. 10.

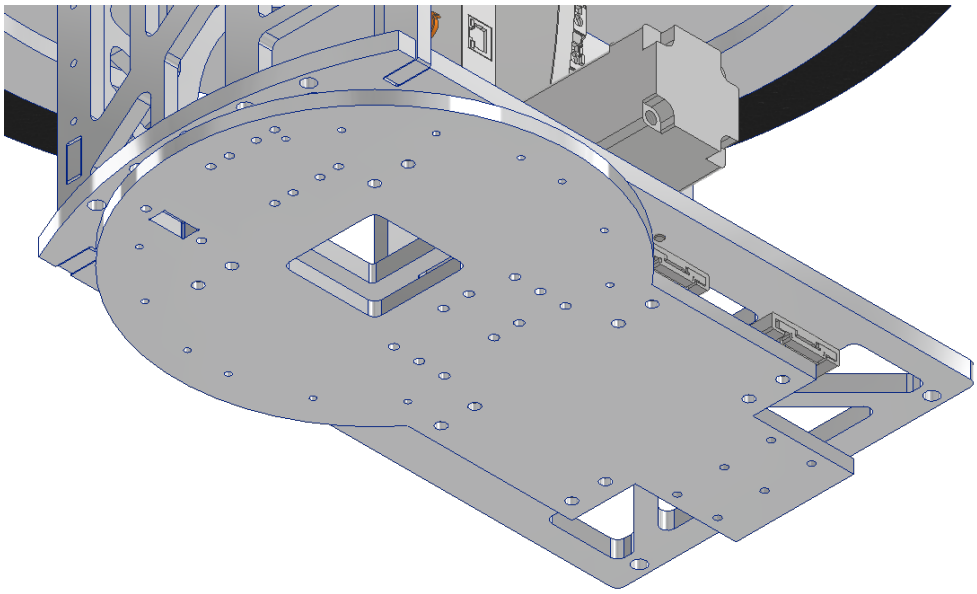

Fig. 9. Linear master y-axis with mounting holes for laser optics, wire axis, and accessories.

1) Wire Linear axis: In order to move the wire in x, y, and z axis without moving the laser spot, a series of adapters were designed and manufactured to motorize the linear guides and minimize the total footprint. These axis were in turn mounted on the previously mentioned laser fixture and are therefore able to move both together with the laser spot and independently. The adapters, guides, and more can be seen in Fig. 10.

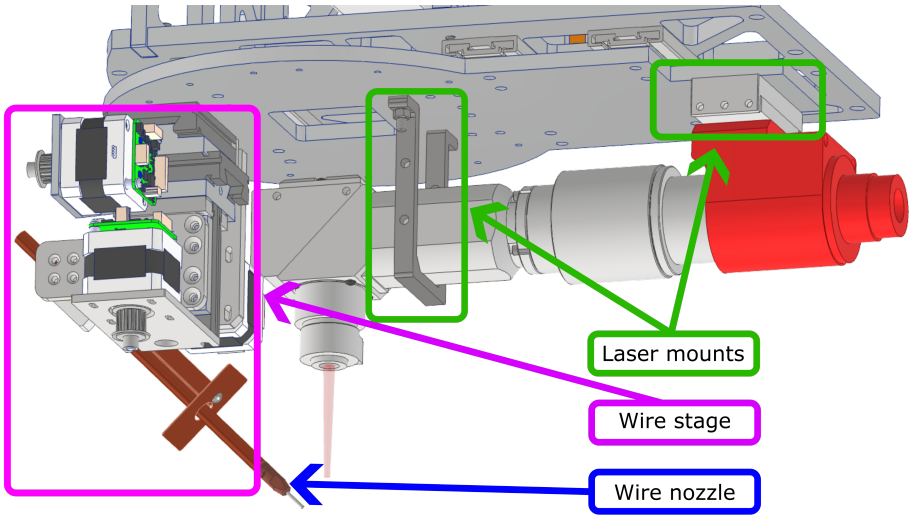

Fig. 10. Full CAD assembly of the system before physical construction.

Wire-feeder The lower deposition rate and smaller size of the features requires a more precise wire feeding system than previously used. As Lw-DED is closely related to laser welding, a wire feeder for laser welding was previously used but proved to have too much backlash for this application. A modified version with custom electronics was developed in order to move the feeder as close as possible to the nozzle to minimise the amount of wire that can cause backlash.

Conductance sensor mount The mount for the conductance sensor had to be manufactured in a non-conductive material as it required galvanic isolation from the rest of the system. The final design was therefore sintered in nylon for improved temperature resistance and dimensional accuracy after prototyping designs in PLA and PETG.

C. Process evaluation

To verify that the process and tool provide an improvement in accuracy and allows for fine detail, three different tests were conducted. The tests were single bead on edge, dual bead on edge, and 'brick on face'. All of the tests were conducted with SS308LSi 0.8 mm wire but with varying substrates.

The produced geometry should be near net shape but not smaller. A larger geometry is allowed as this can be handled in post processing. The application demands that the produced features are 100 % dense with no lack of fusion defects as these can be a source for fatigue failures. The single bead on edge sample is in focus, as jet turbine blade repair is the focus of the report and single bead on edge is a promising method for this. Dual bead on edge is also important but is mainly used to correctly tune parameters as this is regarded to be an easier feature to produce.

Single bead on edge is where single bead layers are repeatedly deposited on the edge of the plate in order to progressively build a wall wider than net shape. The plate used will be 1 mm thick and made of stainless steel. This process is the most complex as it's prone to undercuts and excessive heat buildup. It is also much less forgiving to process disruptions as a small interruption can propagate higher up. As this is the most complex test with the most research value it, in addition to cross section analysis with optical microscope, is scanned with computed tomography (CT) in order to ensure that density and defect requirements are met.

Dual bead on edge is where two beads are positioned next to each other on a plate edge. However this method can easily produce lack of fusion defects in the transition between the weld beads if improper wetting occurs or if the welds are too far away from each other leaving small voids. In Fig. 11 the arrangement of deposited beads can be seen. Here the laser optic is angled to the side to get higher laser absorption into the previous bead to improve wetting. The dual bead on edge sample was cut into three cross sections perpendicular to the layers, etched, and polished to check for defects using an optical microscope.

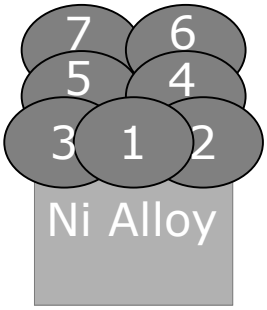

Fig. 11. Schematic view of the bead arrangement in dual bead on edge, note that the bottom layer has three layers to mitigate undercut.

Brick on face is used to evaluate the process capabilities of features with higher heat absorption. Hence, a company standard test coupon was created. The size of these coupons is 4 layers wide

and 10 layers high in a straight line creating a ’brick’. The substrate was the face of a 2 mm thick Inconel 718 alloy plate. The coupon was analyzed using the same method as for the dual bead on edge sample.

III. Results

A. *Test Results*

The single bead on supported edge sample, was CT scanned at PTC in Trollhättan with a Phoenix V|tome|x M240 with a 240 kV microfocus X-ray source and a 180 kV nanofocus X-ray source resulting in a voxelsize of 2 µm. Using the standard sensitivity threshold of 25 % the scan showed zero defects and 100 % density. The threshold was then progressively lowered to 10 % in order to show any possible defects. The volume of the potential defects as listed in Table II indicates that the potential defects are lack of fusion while providing a 100 % dense part. Metallographic preparation and microstructure analysis using light optical microscopy, presented in Figs. 12, 13, 15-17a, as well as 21 and 22 in Appendix E were performed by Dr Almir Heralic at Procada. The CT scan and related images were prepared by Procada at Produktionstekniskt Centrum (PTC).

Fig. 12 and 13 shows that the produced geometry is larger than net shape in all areas. The potential defects can be found in appendix C with the largest one singled out in Fig. 19b. In Fig. 12, a cut and and etched single bead wall sample imaged with optical microscope shows the melt penetration between the layers as well as the microstructure.

TABLE II
A SUMMARY OF FOUND DEFECTS FROM CT SCANNING THE SINGLE BEAD WALL WITH CERTAINTY PROBABILITY ABOVE 10%. THE FULL VERSION IS LOCATED IN APPENDIX B.

Probability	**Radius [mm]**	**Diameter [mm]**	**Equivalent diameter [mm]**	**Volume [mm³]**
21.89	0.025	0.050	0.024	0.000
20.24	0.011	0.022	0.014	0.000
14.75	0.009	0.019	0.012	0.000
14.71	0.012	0.024	0.011	0.000
12.79	0.010	0.021	0.015	0.000
12.61	0.016	0.033	0.017	0.000
12.31	0.014	0.027	0.015	0.000
11.69	0.013	0.026	0.015	0.000
11.35	0.010	0.021	0.013	0.000
10.53	0.012	0.024	0.014	0.000
10.37	0.009	0.018	0.012	0.000
10.15	0.010	0.020	0.013	0.000
10.05	0.019	0.038	0.018	0.000
10.02	0.009	0.018	0.011	0.000

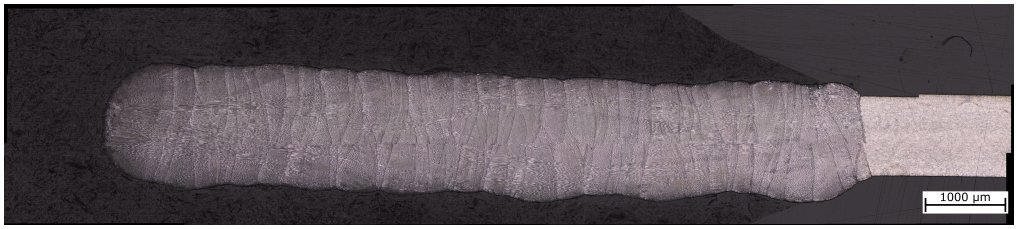

Fig. 12. Cross sectional image of a etched single bead on supported wall sample.

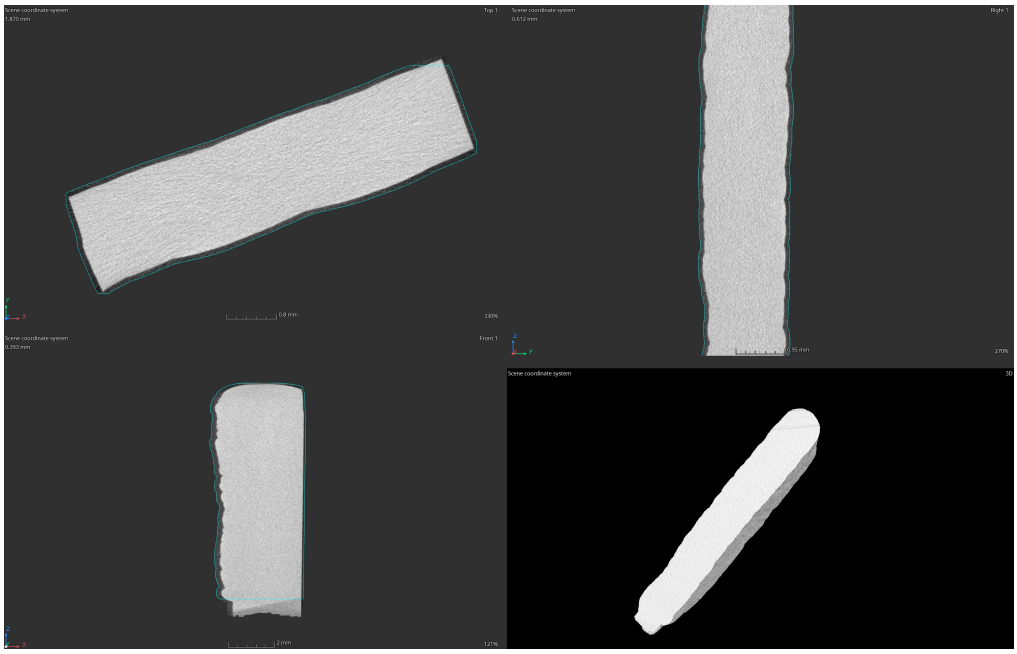

Fig. 13. Images showing different angles from the CT scan of the single bead on supported edge sample.

The dual bead on supported edge sample displays both lack of fusion in the first half of the built wall and proper fusion in the second half as seen in Fig. 14. However, when observing the cross section scans seen in Fig. 15 and 16, several crack formations can be seen in the initial layers.

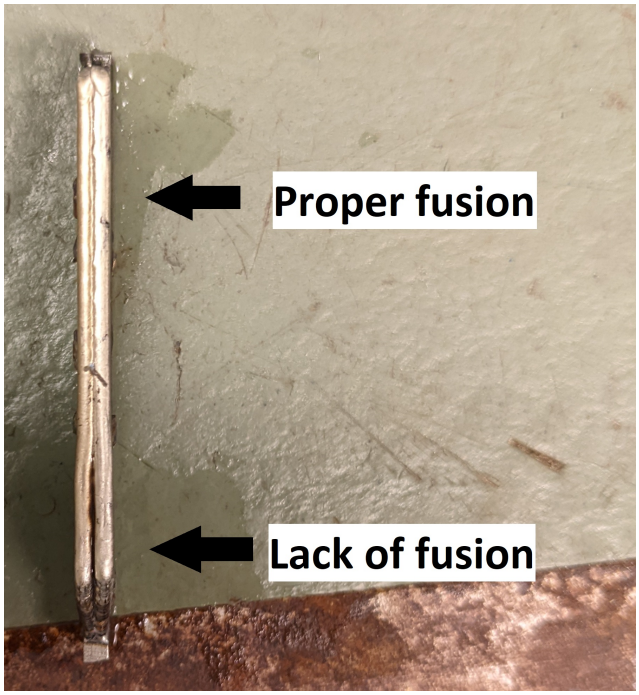

Fig. 14. Image showing a top-down view of the dual bead on supported edge sample with visible distinct sections of lack of fusion and proper fusion.

Fig. 15. Three cross section scans of dual bead on supported wall shown in Fig. 14 stitched together.

Fig. 16. Enlarged image of the first cross section in Fig. 15 showing voids/cracks in the initial layers where SS308LSi and Inconel 718 are mixed.

The brick on face sample showed multiple defects in the initial layers, similar to the case with the dual bead on supported edge. This sample also contains a major void as seen in Fig 17a. A small void can be seen to have formed in during the process as seen in Fig 17b. Additional images are available in Appendix E. Additionally, when measuring the sample, the resulting dimensions, excluding length, were 2.50 mm thick and 3.46 mm wide. This gives an average net layer height of 0.25 mm with a set layer height of 0.20 mm and layer width of 0.88 mm using 0.8 mm thick wire.

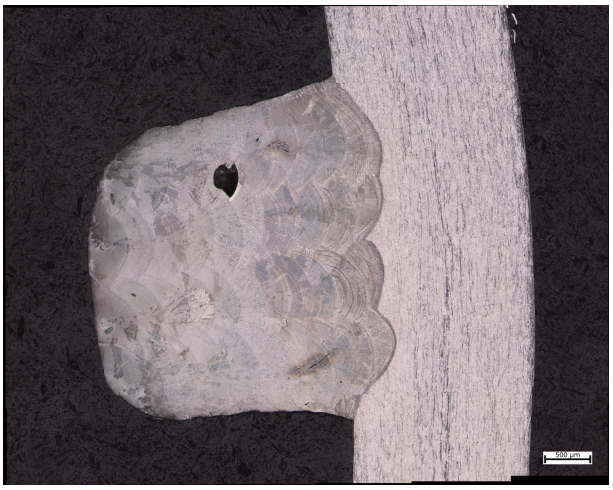

(a) Cross section image of the test coupon showing a void defect around layer 7.

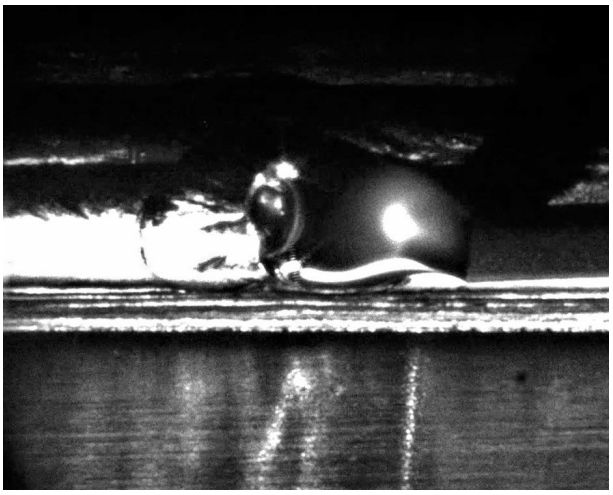

(b) Process image showing the potential moment the void defect occurred.

Fig. 17. Cross section and process images of the brick on face sample.

B. Discussion

The obtained results are opening a new horizon for repair of aerospace components. As this thesis contained creation of the tool used, there was limited time to produce results with different materials and more optimised parameters. As many jet turbine blades are made of titanium alloys, this would have been interesting to examine and would have produced smoother surface finish in part due to the comparably lower viscosity of a titanium melt pool. In addition, only simple geometries were produced even tough the tool should be capable of creation of more advanced geometries.

As a result of the small wire and spot size with a feed rate of 4.2 mm/s, the current deposition rate during testing was relatively low, around 7.6 cm^3/h as calculated with equation (1), compared to a larger scale Lw-DED process which is up to 2500 cm^3/h [8]. This puts the tool closer to the deposition rate of powder based systems rather than more standard Lw-DED. In the potential applications for this process, this deposition rate may however still be advantageous as the single bead walls are slightly above net shape making the process highly efficient. Furthermore, the deposition rate is calculated from early testing and therefore has a high potential to improve with time.

$$V = f \cdot \pi \cdot R^2 \cdot 3.6 \tag{1}$$

While the system is highly rigid and has a resolution of about 50 μm it is somewhat lacking in acceleration and speed. In large part this is due to the linear motion systems chosen as they use aluminum dovetails and fine pitch M5 rods, this means that the friction both in the guide ways and threads are higher than in a system with components more adapted for motor control. An example of a more suited but similar system would be to have linear rails coupled with ball screws to achieve less friction with negligible changes in rigidity. Another interesting alternative to investigate is the use of flexures for motion translation as this has potential for even higher rigidity.

Looking at the test results from the single bead on supported edge shows very promising results with no defects at standard measuring confidence. With the addition of being larger than net size this has potential as a way to repair jet engine turbine blades.

However, the dual bead on supported edge and brick on face both showed a high occurrence of defects in the initial layers as seen in Fig. 15, 16 and Appendix E, as well as the brick showing a large void in Fig. 17b. The suspected reason for the defects in the initial layers is due to having too short cooling periods between passes in the layers where the SS308LSi filler mixed with the Inconel 718 base. Therefore, the defects are a result of the chosen process parameters, rather than from the overall process itself. Thus they are expected to be solved with further experience and optimization.

The void is thought to be the result of a process interruption. There might be some contamination present or melt pool instability. When inspecting the recorded footage there might be some minor stubbing as the wire was located just on the surface of the substrate during the process. Whatever the cause this resulted in a non-uniform distribution of material that propagated upwards until the moment of Fig. 17b where the new layer encountered the discontinuity creating a void. This issue is thought to be corrected by iterating the correct process parameters as this was not a problem in the single bead.

1) Further improvements: Currently, the only fully automatic controls of the system, aside from the robot arm, is the wire height and speed. The rest are manually tuned during the process. Thus, automating the rest of the implemented systems would be a future programming challenge to allow

for more complex geometry and a more repeatable process without human interference. The hardware and codebase to allow for this is available but not fully integrated.

Another improvement would be in the wire positioning system, to design and construct a more appropriate solution instead of a retrofitted manual system. For example linear guide rails with ball screws instead of dovetail linear guides with threaded rod.

Since the tool features a higher resolution at the cost of deposition rate, a potential further improvement may be to combine the system with one using a larger diameter wire to give the option to switch between high resolution and high deposition rate in the same job. For context, in Appendix D, a comparison between single wall depositions from the new tool compared to the old tool can be seen.

2) Further research: Further research of the process should include evaluation of the build quality and effect of further process window improvements by using smaller wire. The impact of different quality wire on said process window should also be investigated. There is also further research needed in why, and how, the defects seen in multi-wall features occur and can be prevented. Another thing to look at is the use of other filler materials than SS308LSi.

C. Conclusion

This thesis has implemented a tool capable of producing smaller features than previously possible by the Lw-DED process. The enabler for this is the reduction in size of the laser spot and wire diameter. The main additions to the tool presented in this thesis compared to other tools designs is the ability to position the wire in three dimensions. As well as the ability to follow seams more accurately than before by using a linear stage to allow for seam following. In addition, improvements to the process parameters has also been made to accommodate for this smaller size.

The single wall parts produced can be assumed to feature a 100 % density as the default probability threshold had to be lowered to find any potential defects. These repairs would be possible to apply in high fatigue environments such as in the repair of jet engine fan blades. Therefore, the tool and produced parts show excellent potential for repair of jet engine turbine blades. However, further improvements to the process needs to be done to features requiring multiple walls.

The feature layer height is in the range of 0.18 mm to 0.25 mm and a layer width of 1.35 mm to 1.59 mm when using 0.8 mm SS308LSi wire, with potential to go even finer by using an even smaller wire diameter. Compared to processes using wire with a larger diameter, it has been found that when reducing the diameter, the process was more sensitive to stubbing and droplet formation as an effect of the change in cross sectional area.

The tool is capable of fine adjustment of the wire position relative to the laser spot position as well as adjustment of the laser spot orthogonal to the feed direction and z-axis. Together with the mounted optical system and sensors, the system is ready for implementing a sensor fusion based automatic control loop to further improve the process window and allow for more complex geometry production.

APPENDIX A

IMAGE OF THE COMPLETE TOOL.

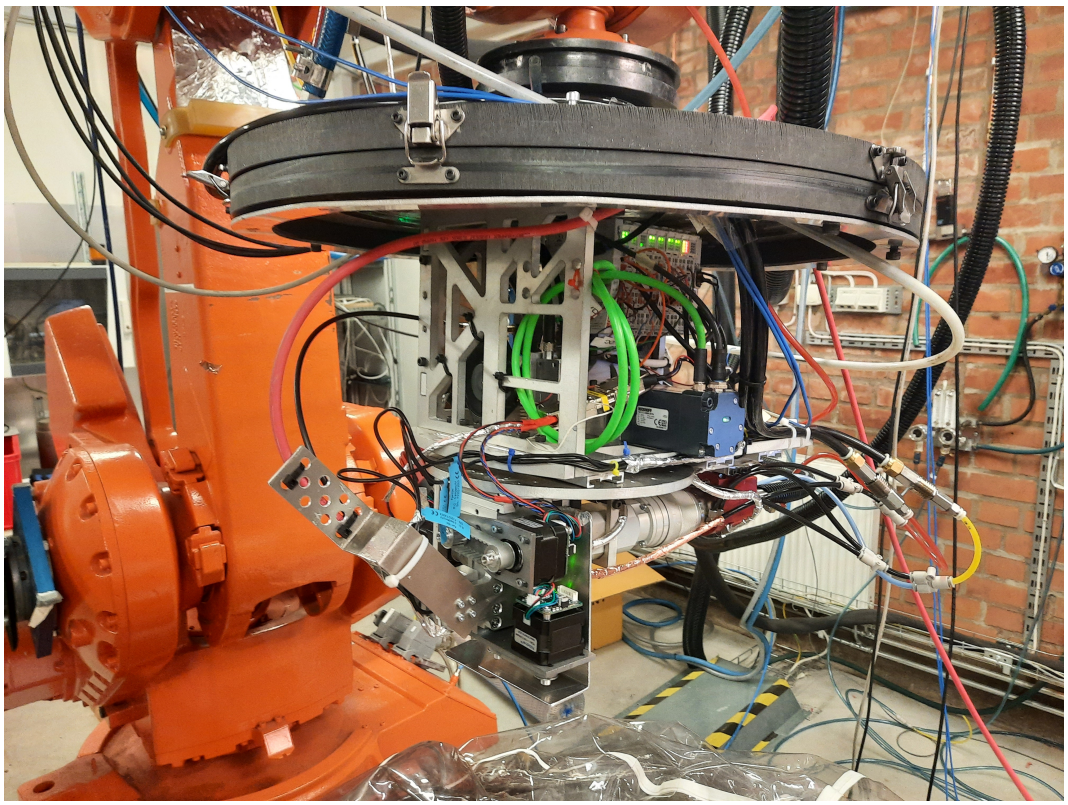

Fig. 18. Image showing the full assembled system absent a gas tent.

APPENDIX B

COMPLETE TABLE OF CT SCAN RESULTS.

Probability	Radius [mm]	Diameter [mm]	Equivalent diameter [mm]	Volume [mm³]	Surface [mm²]	Gap [mm]	Compactness	Sphericity	Projected size x [mm]	Projected size y [mm]	Projected size z [mm]	PCA deviation 1 [mm]	PCA deviation 2 [mm]	PCA deviation 3 [mm]	PCA max. deviation ratio [%]	PCA min. deviation ratio [%]	Min. gray value	Max. gray value	Mean gray value	Deviation of gray values
21.89	0.025	0.050	0.024	0.000	0.002	0.323	0.11	0.73	0.053	0.020	0.026	0.010	0.007	0.004	41.78	15.89	30812	42433	38423	2781
20.24	0.011	0.022	0.014	0.000	0.001	0.644	0.27	0.83	0.026	0.013	0.013	0.005	0.004	0.003	43.81	32.08	32261	40860	37830	2576
14.75	0.009	0.019	0.012	0.000	0.001	0.546	0.27	0.80	0.026	0.013	0.013	0.006	0.004	0.003	62.05	26.55	33086	40178	37944	2405
14.71	0.012	0.024	0.011	0.000	0.001	0.930	0.11	0.65	0.026	0.007	0.020	0.006	0.004	0.002	54.65	14.01	33180	39794	37105	2562
12.79	0.010	0.021	0.015	0.000	0.001	0.644	0.35	0.83	0.026	0.013	0.020	0.005	0.005	0.003	49.52	30.94	35118	40993	38218	1858
12.61	0.016	0.033	0.017	0.000	0.001	0.323	0.13	0.73	0.040	0.020	0.020	0.010	0.004	0.003	60.01	19.41	34217	41469	39401	2198
12.31	0.014	0.027	0.015	0.000	0.001	3.198	0.16	0.69	0.026	0.013	0.026	0.008	0.005	0.002	57.99	17.95	33796	41407	37843	2348
11.69	0.013	0.026	0.015	0.000	0.001	0.455	0.20	0.74	0.026	0.013	0.020	0.005	0.005	0.003	41.55	22.85	35516	42002	39348	1954
11.35	0.010	0.021	0.013	0.000	0.001	0.872	0.23	0.76	0.013	0.013	0.020	0.006	0.004	0.003	57.39	24.56	34920	40225	37600	2087
10.53	0.012	0.024	0.014	0.000	0.001	1.382	0.20	0.73	0.026	0.013	0.020	0.005	0.005	0.003	41.07	26.98	32844	39010	36888	2111
10.37	0.009	0.018	0.012	0.000	0.001	0.455	0.28	0.76	0.026	0.007	0.020	0.005	0.004	0.002	60.53	18.44	35223	41665	39431	2092
10.15	0.010	0.020	0.013	0.000	0.001	0.930	0.27	0.78	0.026	0.020	0.020	0.005	0.004	0.004	48.43	35.04	32664	40979	38986	2399
10.05	0.019	0.038	0.018	0.000	0.002	0.546	0.11	0.65	0.040	0.020	0.026	0.009	0.005	0.003	48.03	18.39	34744	41367	38482	2133
10.02	0.009	0.018	0.011	0.000	0.001	0.872	0.19	0.68	0.026	0.007	0.013	0.005	0.003	0.002	58.73	18.04	32957	39199	37207	2247

TABLE III

RAW DATA FROM CT SCAN OF THE SINGLE BEAD WALL.

APPENDIX C

IMAGES FROM CT SCAN OF SINGLE BEAD ON SUPPORTED EDGE.

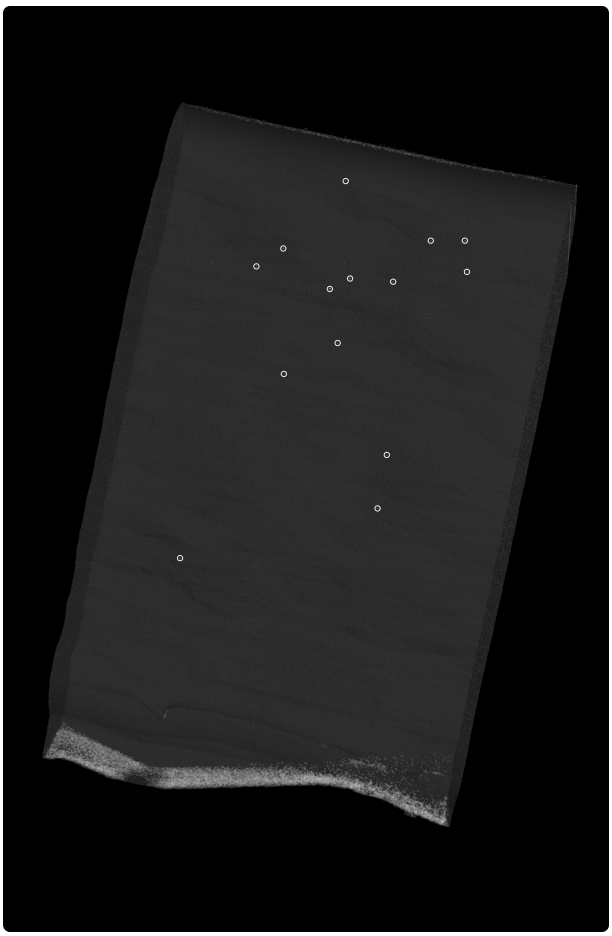

(a) CT scan at 10 % probability threshold with possible defects circled in white.

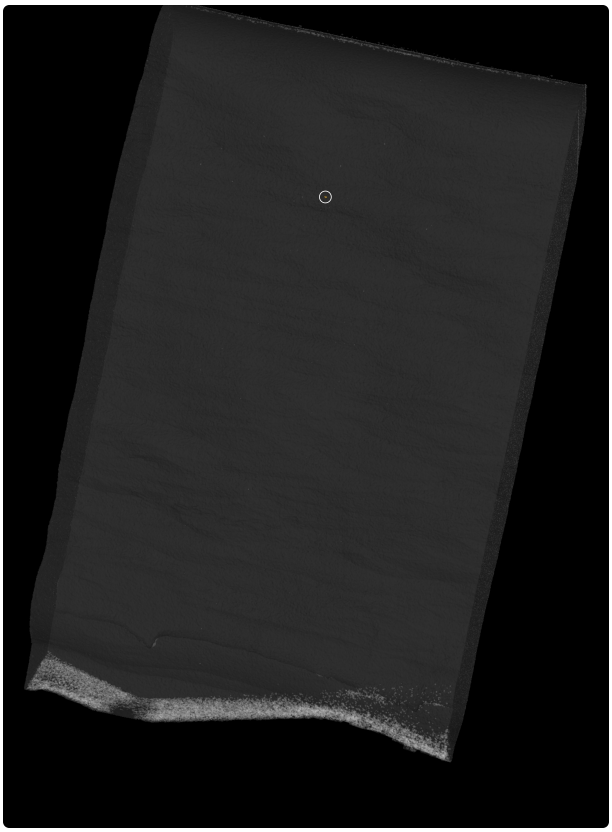

(b) CT scan at 10 % probability threshold with only the largest possible defects circled in white.

Fig. 19. CT scan images at 10 % threshold with all and only the largest defects respectively circled in white.

APPENDIX D

CROSS SECTIONAL IMAGE OF SINGLE BEAD ON SUPPORTED EDGE COMPARISON

Fig. 20. Comparison of cross section scans from single bead walls created by the new tool in SS308LSi and old tool in Ti6Al4V. Comparison sample provided by Procada [3].

APPENDIX E

CROSS SECTIONAL IMAGES OF THE BRICK ON FACE

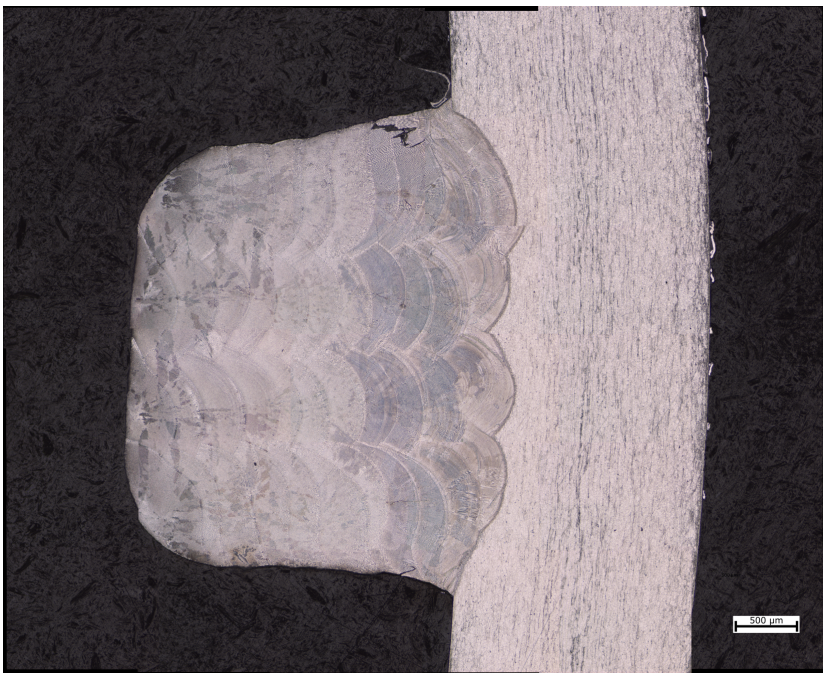

Fig. 21. Cross section image of brick on face sample showing potential defects in the transition zone around the initial layers reaching the outer edge. It is noted however that this may be due to contamination of the sample.

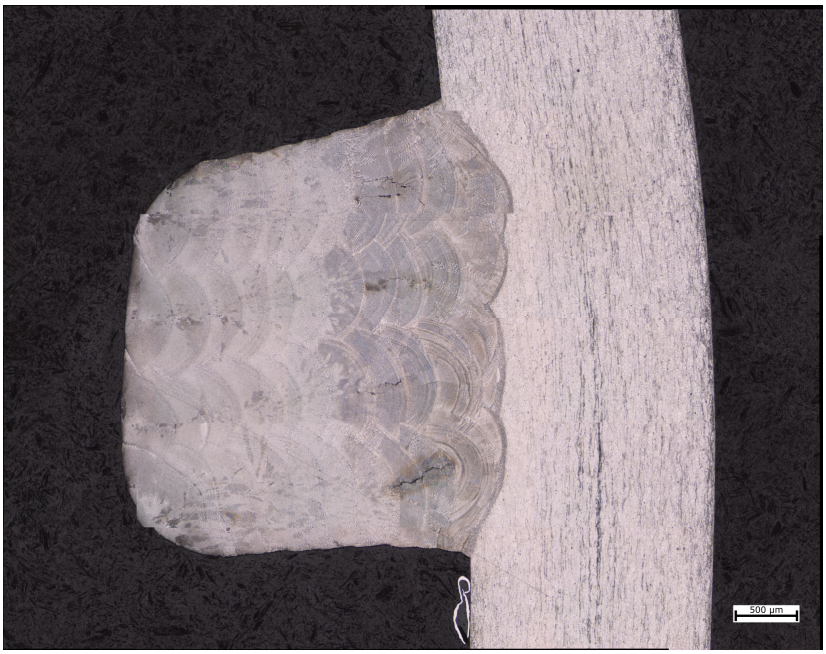

Fig. 22. Cross section image of brick on face sample showing potential defects in the initial layers where SS308LSi mixed with Inconel 718.

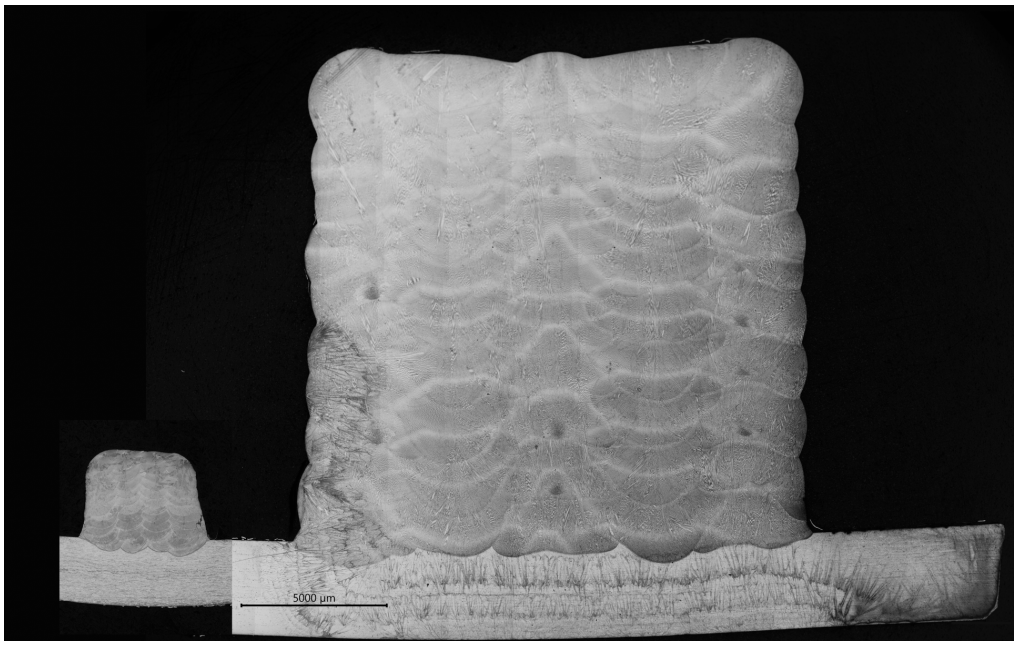

Fig. 23. Cross section image of brick on face sample in SS308LSi produced with the new tool (left) compared to a brick on face cross section of the old process using Inconel 718 with 10 layers and 5 beads (right). Comparison sample provided by Procada [3].

References

[1] NASA, *Principles of Directed Energy Deposition for Aerospace Applications*, 2021. [Online]. Available: https://ntrs.nasa.gov/api/citations/20210000449/downloads/UTEP-Course%20-%20Principles%20of%20DED_Gradl_Jan2021.pdf, visited on 03/07/2022.

[2] R. B. Wei Guo, "Business case for repair via ded processes and best practice for classification and qualification of component damage.," 2018. [Online]. Available: https://ec.europa.eu/research/participants/documents/downloadPublic?documentIds=080166e5b83899e5&appId=PPGMS, visited on 05/31/2022.

[3] Procada AB, *procada website*, 2022. [Online]. Available: https://procada.se/technology.html, visited on 03/07/2022.

[4] "Standard guide for directed energy deposition of metals," American Society for Testing and Materials, Standard, Dec. 2016.

[5] I. Gibson, D. Rosen, and B. Stucker, *Additive Manufacturing Technologies*. 2010. [Online]. Available: https://doi.org/10.1007/978-1-4419-1120-9.

[6] A. HERALIC and P. HAGQVIST, "Additive manufacturing," EP3831525A1, Dec. 2019. [Online]. Available: https://patents.google.com/patent/EP3831525A1/.

[7] A. Heralic, "Towards full automation of robotized laser metal-wire deposition," Jan. 2009. doi:https://www.diva-portal.org/smash/get/diva2:287573/FULLTEXT01.pdf.

[8] D. Ding, Z. Pan, D. Cuiuri, and H. Li, "Wire-feed additive manufacturing of metal components: Technologies, developments and future interests," *International Journal of Advanced Manufacturing Technology*, vol. 81, May 2015. doi:10.1007/s00170-015-7077-3.

[9] W. U. H. Syed and L. Li, "Effects of wire feeding direction and location in multiple layer diode laser direct metal deposition," *Applied Surface Science*, vol. 248, no. 1, pp. 518–524, 2005, 4th International Conference on Photo-Excited Processes and Applications, ISSN: 0169-4332. doi:https://doi.org/10.1016/j.apsusc.2005.03.039. [Online]. Available: https://www.sciencedirect.com/science/article/pii/S0169433205004344.

[10] trinamic, *Pd42-1140 product page*, 2022. [Online]. Available: https://www.trinamic.com/products/drives/details/pd42-x-1140/.

INDUSTRIAL AND MATERIALS SCIENCE
CHALMERS UNIVERSITY OF TECHNOLOGY
Gothenburg, Sweden
www.chalmers.se

CHALMERS
UNIVERSITY OF TECHNOLOGY